

Citation for published version:

Svensson, C, Hannford, J & Prosdocimi, I 2017, 'Statistical distributions for monthly aggregations of precipitation and streamflow in drought indicator applications', *Water Resources Research*, vol. 53, no. 2, pp. 999-1018.
<https://doi.org/10.1002/2016WR019276>

DOI:

[10.1002/2016WR019276](https://doi.org/10.1002/2016WR019276)

Publication date:

2017

Document Version

Peer reviewed version

[Link to publication](#)

University of Bath

Alternative formats

If you require this document in an alternative format, please contact:
openaccess@bath.ac.uk

General rights

Copyright and moral rights for the publications made accessible in the public portal are retained by the authors and/or other copyright owners and it is a condition of accessing publications that users recognise and abide by the legal requirements associated with these rights.

Take down policy

If you believe that this document breaches copyright please contact us providing details, and we will remove access to the work immediately and investigate your claim.

Statistical distributions for monthly aggregations of precipitation and streamflow in drought indicator applications

Cecilia Svensson^{1,*}, Jamie Hannaford¹, Ilaria Prosdocimi^{1,2}

¹ Centre for Ecology & Hydrology, Maclean Building, Benson Lane, Crowmarsh Gifford, Wallingford, Oxfordshire, OX10 8BB, UK

² Now at the Department of Mathematical Sciences, University of Bath, Claverton Down, Bath, Somerset, BA2 7AY, UK

* Corresponding author, email: csve@ceh.ac.uk

15 September 2016

Running title: Statistical distributions for precipitation and streamflow

Key points

The suitability of twelve statistical distributions for characterizing long-duration precipitation and streamflow data was evaluated

The novel and flexible three-parameter Tweedie distribution has a lower bound at zero and describes the data well

The Tweedie distribution is advocated for calculation of precipitation and streamflow drought indices

Abstract

Drought indicators are used as triggers for action and so are the foundation of drought monitoring and early warning. The computation of drought indicators like the standardized precipitation index (SPI) and standardized streamflow index (SSI) require a statistical probability distribution to be fitted to the observed data. Both precipitation and streamflow have a lower bound at zero, and their empirical distributions tend to have positive skewness. For deriving the SPI, the Gamma distribution has therefore often been a natural choice. The concept of the SSI is newer and there is no consensus regarding distribution. In the present study, twelve different probability distributions are fitted to streamflow and catchment average precipitation for four durations (1, 3, 6, and 12 months), for 121 catchments throughout the United Kingdom. The more flexible three- and four-parameter distributions generally do not have a lower bound at zero, and hence may attach some probability to values below zero. As a result, there is a censoring of the possible values of the calculated SPIs and SSIs. This can be avoided by using one of the bounded distributions, such as the reasonably flexible three-parameter Tweedie distribution, which has a lower bound (and potentially mass) at zero. The Tweedie distribution has only recently been applied to precipitation data, and only for a few sites. We find it fits both precipitation and streamflow data nearly as well as the best of the traditionally used three-parameter distributions, and should improve the accuracy of drought indices used for monitoring and early warning.

Index terms

1816 Estimation and forecasting

1854 Precipitation

1860 Streamflow

1804 Catchment

Keywords

Standardized precipitation index, standardized streamflow index, statistical distribution, Tweedie distribution, drought index, United Kingdom.

1. Introduction

It is widely written that drought is a complex phenomenon that is notoriously hard to define. The challenges of drought definition have been acknowledged for at least 30 years, certainly since *Wilhite and Glantz* [1985], and recently *Lloyd-Hughes* [2014] argued that a universal definition is simply impracticable. Given the vagueness of the concept of drought, it is perhaps unsurprising that there has been a proliferation of drought indicators over the last two decades: *Lloyd-Hughes* [2014] counted over 100 different indicators, with no sign of abatement in this trend in the international literature. While there is some merit in applying different indicators for different purposes – recognizing the widely acknowledged multifaceted nature of the drought hazard, from meteorological, hydrological, agricultural, socio-economic, etc – there is also benefit in seeking indicators that are consistent and comparable. Indicators provide crucial information to support the recognition of drought onset and termination, and thus duration, as well as the relative severity and rarity of events. They are used as triggers for action and communication (or declaration of drought) and so are the foundation of drought monitoring and early warning.

One of the more popular indicators, now recommended by the World Meteorological Organization (WMO) [*Hayes et al.*, 2011] as an indicator for meteorological drought, is the Standardized Precipitation Index (SPI) first formulated by *McKee et al.* [1993], see section 3.4 for details. A key advantage of the SPI is that, by virtue of the standardization process, it enables comparison between locations and between different times of year. It is also flexible in that it can be aggregated across a range of timescales (e.g. 1, 3, 6, 12 months), which are relevant for different types of drought impacts. As such, the SPI has been widely applied in monitoring and early warning systems (e.g. see the review by *Bachmair et al.*, 2016) and is extensively used for other purposes.

While the SPI is widely seen as a de facto indicator of choice, it is not without limitations. By construction the SPI is inherently sensitive to the time period used for standardization, and the choice of statistical distribution used to effect the transformation to a normal distribution. The impact of record length and standardization period has been analyzed [e.g. *Wu et al.* 2005, *Núñez et al.*, 2014]. The choice of distributions has been discussed since the early days of the SPI; the question is far from academic and can have major implications for drought severity and characteristics. The original paper [*McKee et al.*, 1993] employed the gamma distribution, and this has been widely adopted and is sometimes seen as a default; it has

generally been shown to perform relatively well across most of Europe [Lloyd-Hughes and Saunders, 2002]. However, a later systematic test across Europe [Stagge *et al.*, 2015] found that while the Gamma distribution could still broadly be recommended as a default, other distributions perform better in some areas, and at some aggregation timescales. Other authors have noted limitations with the Gamma distribution, in particular under (over) estimation of wet (dry) extremes [e.g. Sienz *et al.*, 2012]. Some authors [e.g. Guttman, 1999] have advocated three parameter distributions such as the Pearson Type 3 as more flexible alternatives.

In the last decade there has been an increased interest in the application of the SPI concept to other domains of the hydrological cycle. A Standardized Precipitation and Evapotranspiration Index (SPEI), developed by Vicente-Serrano *et al.* [2010] has become very popular, and other studies have sought to apply standardization to runoff [Shukla and Wood, 2008], streamflow [e.g. Vicente-Serrano *et al.* 2012], groundwater [Bloomfield and Marchant, 2013] and snowmelt [Staudinger *et al.*, 2014]. Finding suitable distributions is as important for these variables as it is for the SPI, but this topic has been relatively under-researched. Unlike for the SPI and SPEI, for streamflow there is not even a broad consensus on the most appropriate distributions to use. For the standardized streamflow index (SSI), there are only a few published studies (to the authors' knowledge) that address choice of distribution, and they all tend to focus on a limited number of sites or a localized geographical domain. Vicente-Serrano *et al.* [2012] examined distributions for 98 sites in the Ebro basin in Spain, finding that no distribution worked best, partly due to the substantial variations in streamflow regimes, even over a relatively limited area. These authors instead advocate an approach of empirically choosing best distributions for each month and location. Soláková *et al.* [2014] examined a range of distributions for a single site in Italy, compared to a non-parametric approach. For groundwater, the Standardized Groundwater Index (SGI) [Bloomfield and Marchant, 2013] has been developed using a non-parametric approach due to the inappropriateness of most distribution fits for a range of boreholes in the UK. For meteorological data covering larger areas, most of the systematic tests of distributions have been applied to readily-available, continuous gridded datasets, e.g. Stagge *et al.* [2015] for Europe, rather than to catchment observations.

The aim of this paper is to systematically test distributions for application to the SPI and SSI using a large dataset of 121 near-natural catchments across the whole of the UK, with respect to

- 1) goodness-of-fit and general distributional behavior, including visual inspection of the fitted probability density functions,
- 2) the degree to which unbounded distributions have mass below zero (as hydrological data have a lower bound at zero),
- 3) effects of seasonality and catchment characteristics on the goodness-of-fit.

One immediate purpose of the study is to provide guidance for application of such standardized indicators in the UK; the SPI has not been routinely employed beyond a few research studies [e.g. *Hannaford et al.* 2011; *Bloomfield and Marchant*, 2013; *Folland et al.* 2015], with the SSI even less so. Standardized indices are not routinely used in drought monitoring and early warning (with the exception of in Scotland, where an SPI variant is used [Gosling, 2014]), but there is increasingly an appetite for consistent indicators for drought definition [e.g. *Collins et al.*, 2015]. There is a pressing need to tackle this question, given the diversity of catchment types seen in the UK, to provide recommendations for application of the SPI and SSI in monitoring and early warning systems and other applications. A related paper [Barker et al., 2016] further tests the utility of the SPI and SSI in the UK, using them to investigate the propagation from meteorological to hydrological drought and relating the propagation characteristics to catchment characteristics. By virtue of the scale of the dataset and diversity of climatic and landscape characteristics seen in the UK (as discussed in Barker et al., [2016]), we envisage the test application presented here could be of wide international relevance, given the paucity of studies that have addressed comprehensively the question of distribution choice for both precipitation and river flow in parallel.

2. Data

2.1 Precipitation and streamflow data

Monthly mean streamflow and precipitation data for 121 catchments in the UK benchmark network were used for the analysis. The benchmark network comprises catchments with near-natural river flow regimes and long, good-quality flow records [Bradford and Marsh, 2003]. Here, “near-natural” is defined as catchments having minimal net influence of abstractions, discharges or impoundments. The benchmark catchments are located throughout the country (Figure 1a), and can be considered to be representative of the range of catchment conditions encountered across the UK. The catchment areas vary between 3.07 and 4587 km² (Figure

1b). The selected catchments have at least 30 years of both river flow and precipitation records within the period October 1929 to September 2014 (Figures 1c and 1d).

Daily mean streamflow and catchment average monthly precipitation totals were provided by the National River Flow Archive (NRFA) [Marsh and Hannaford, 2008]. For streamflow, each individual month was required to have at least 25 days of valid daily mean flow observations for a monthly mean flow (expressed in m^3/s) to be calculated and used in this study. The mean and median record lengths are 47.3 and 44.9 years, respectively, when missing data are included. Almost half of the catchments (59 of 121) have complete records between their individual start and end dates, and the remainder has on average 2.7% missing data. The longest record, for the Dee at Woodend in northeast Scotland, spans the whole 85-year period October 1929 to September 2014 and has no missing data. There were two ephemeral streams in the initial catchment selection, with 4% and 13% of monthly flows equal to zero. Because of this relatively large amount of zeroes in the dataset, these catchments were removed so that all monthly flow observations for the selected 121 catchments exceed zero. This was done to avoid the complication of treating the data for some catchments differently to the rest, and to enable a straightforward comparison of the proposed distribution functions. It also avoids having to distinguish between instances of a zero flow recording because of a lack of rainfall, and because of frozen conditions (although the latter tend not to be long-lasting in the UK).

The periods of record for the catchment average monthly precipitation data differ slightly from those for the streamflow records, with mean and median record lengths being slightly longer, at 47.8 and 46.6 years, respectively. However, the precipitation records for all catchments end in December 2012, nearly two years before the last river flow record. The longest record is again the one for the Dee at Woodend, starting in October 1929 and ending in December 2012, without any missing data. Only four of the catchments have missing precipitation data between their individual start and end dates, on average 2.3%. The monthly precipitation totals equaled zero for one month each in four catchments. These single observations were set to 0.01 to avoid having zeroes in the dataset. The monthly precipitation totals were converted to monthly averages expressed in mm/day.

2.2 Catchment descriptors

Indices describing the characteristics of each catchment were also supplied by the NRFA [Marsh and Hannaford, 2008; Bayliss, 1999]. These include catchment AREA, SAAR (the standard average annual rainfall 1961-1990), SMDBAR (the average soil moisture deficit 1960-1990. This is only available for 31 catchments), and BFIHOST, a base flow index which is a measure of catchment responsiveness derived using the 29-class Hydrology of Soil Types (HOST) classification. There is a strong association between BFIHOST and the Baseflow Index derived using a hydrograph separation approach, where the Baseflow Index is a measure of how large the groundwater contribution to streamflow is. Both indices vary between 0 and 1, with higher values indicating a greater contribution of base flow and therefore higher catchment storage, or permeability. Here we consider catchments having BFIHOST values exceeding 0.5 to be permeable and catchments with values less than 0.5 to be impermeable. Most of the permeable catchments are located in the southeast of the UK (see Figure 1a for aquifer outcrop areas).

3. Methods

3.1 Overview

Data series were extracted for each calendar month separately, so that, for example, a series could consist of river flows for January 1965, January 1966, January 1967, and so on. These data series were then transformed to standardized indices: the standardized precipitation index (SPI) for precipitation data and, separately, the standardized streamflow index (SSI) for river flow data. The first step in the transformation was to fit a statistical probability distribution to the data series (e.g. to the series of January river flows). A range of different distributions considered potentially suitable for precipitation and river flow data were tried in this step. Next, the fitted distribution was used to transform the original data to the quantiles of a Normal distribution with mean = 0 and standard deviation = 1. These quantiles, or “normal scores” of the Normal distribution constitute the standardized indices. A range of goodness-of-fit tests were then applied to the standardized indices to investigate which statistical distribution best fitted the original precipitation and river flow data. The novel part of the present study is to systematically test a range of statistical distributions for suitability of describing precipitation and river flow data. In addition to the goodness-of-fit tests, the

mass below zero was assessed for the original distributions, and the influences of seasonality and catchment characteristics on the goodness-of-fits were investigated.

3.2 Aggregated time series

Separate data series were derived for each calendar month, so that series consisting of data for all Januaries were extracted separately from series consisting of data for all Februaries, etc. In addition to these monthly series, longer aggregations of 3, 6 and 12 months were also derived, with separate (backward-looking) aggregated series ending in each of the 12 calendar months of the year. The aggregations are averages of the monthly values in the aggregation duration, so that, for example, the 6-month precipitation aggregation for August 2010 is the average daily rainfall total for March to August 2010. A missing value in one or more of the constituent months of the aggregation leads to a missing value for the total aggregation.

3.3 Statistical distribution functions

In total twelve different probability distributions with two, three or four parameters were considered to be potentially suitable for fitting to the monthly aggregations of precipitation and river flow data (Table 1). Not all of the distributions have a lower bound at zero (like observed precipitation and streamflow do), but unbounded distributions were included in the study as they have been used for deriving standardized indices in the past [e.g. *Guttman*, 1999]. The magnitude of the associated problem of part of the fitted distribution potentially falling below zero is therefore also assessed in the present study.

The sole four-parameter distribution investigated is the Kappa distribution, and the three-parameter distributions include the Generalized Logistic, Pearson type 3, Generalized Extreme Value (GEV) and Tweedie. Of these, only the Tweedie distribution has a lower bound at zero. The two-parameter distributions include the Gamma, Lognormal, Normal, Gumbel and Weibull distributions. Of these, the Normal and Gumbel distributions lack a lower bound. Probably with the exception of the Tweedie, these are all well-known distributions to the hydrologist, and apart from the Tweedie [e.g. *Dunn and Smyth*, 2005] and the Kappa distributions [e.g. *Hosking and Wallis*, 1997], their probability density functions are described in *Stagge et al.* [2015].

In addition, a lower bound at zero was imposed on the three- and four-parameter distributions for which a bounded version of the distribution is not already investigated. That is, a lower bound at zero was imposed for the Generalized Logistic and the Kappa distributions. When such a constraint is applied to the Pearson type 3 distribution, it reduces to the Gamma distribution, which is already included. Similarly, the already included 2-parameter Weibull distribution is a variation of the GEV with a lower bound at zero. The imposition of the lower bound reduces the number of parameters to be estimated by one, so that the three- and four-parameter distributions become two- and three-parameter distributions, respectively. In figures and tables of this paper, the short-hands “GenLog”, “P3”, “Kappa3” and “Kappa4” may be used to denote, in turn, the Generalized Logistic, the Pearson type 3, and the 3- and 4-parameter Kappa distributions.

To the authors’ knowledge the Tweedie distribution has only rarely been applied to hydrological data. *Dunn* [2004] and *Hasan and Dunn* [2011] applied it to monthly rainfalls in Australia, and found that it fitted the data well. The Tweedie is in fact a family of distributions, whose special cases include the Normal ($\xi = 0$), Poisson ($\xi = 1$), Gamma ($\xi = 2$), and Inverse Gaussian ($\xi = 3$) distributions [e.g. *Tweedie*, 1981; *Dunn and Smyth*, 2005]. When the parameter ξ has a value between 1 and 2, the distribution describes series that can contain exact zeroes as well as positive continuous data, whereas for $\xi \geq 2$ the support is for positive continuous data only [*Hasan and Dunn*, 2011]. Although the present study does not include data equal to zero, the Tweedie family of distributions has two attractive features: the lower bound (for $\xi \geq 1$), and that its three parameters make it flexible. Of the other proposed distributions, only the Kappa distribution with a lower bound imposed at zero have both these characteristics. However, a drawback of the Tweedie is that the probability density functions can only be written in closed form for the special cases where ξ equals 0, 1, 2 or 3. For other values of ξ numerical methods need to be used, which makes parameter estimation more time-consuming [e.g. *Dunn and Smyth*, 2008].

Please see Appendix A for further details about the Tweedie distribution, and Appendix B for details about the distribution fitting procedures.

3.4 Transformation to the standardized indices, SPI and SSI

Once distributions are fitted, the observations (i.e. the aggregated series) are transformed to a Normal distribution with mean = 0 and standard deviation = 1, $N(0,1)$, to obtain the

standardized index as described by, for example, *McKee et al.* [1993], *Guttman*, [1999], and *Lloyd-Hughes and Saunders* [2002]. That is, each observation corresponds to a quantile, x , of the fitted cumulative distribution function, $F(x) = P(X \leq x)$, of the distribution of choice (say, for example, the Gamma distribution). By setting

$$F(x) = G(y),$$

where $G(y)$ is the cumulative distribution function of the $N(0,1)$ distribution, the corresponding quantile y of the $N(0,1)$ distribution can be found for each observation. The quantile y , or “normal score”, is the unitless standardized index for the observation, i.e. the SPI or SSI. Hence, the SSI is derived in the same manner as the SPI, but using streamflow rather than precipitation data.

During dryer than average conditions the index will be negative and during wetter than average conditions the index will be positive. Because of uncertainty at the extremes of the distribution, estimates of the index exceeding an absolute value of 5 were truncated and set to the limiting value. Approximately 95% of the calculated indices will occur within the range -2 to +2, and 68% within the range -1 to +1. The exact definitions of different drought severities differ between studies, but spells in the latter range are often denoted as normal to mildly dry/wet, and spells outside the range -2 to +2 as extremely dry/wet.

3.5 Testing the goodness-of-fit

A range of goodness-of-fit tests were applied to investigate how well the different statistical distributions describe the observed data. However, the tests were applied to the transformed indices, rather than to the original precipitation and river flow data. In this way, all the goodness-of-fit tests are applied to normally distributed data with mean = 0 and standard deviation = 1, and the results are straightforward to compare.

The tests include the Shapiro-Wilk test, the Anderson-Darling test, the Cramér-von Mises test and the Kolmogorov-Smirnov test. The Anderson-Darling test is a modification of the Cramér-von Mises test, giving more weight to the tails of the distribution [e. g. *Farrell and Rogers-Stewart*, 2006]. *Razali and Wah* [2011] compared the power of several tests, and concluded that of the four tests investigated the Shapiro-Wilk test was the most powerful test for normality closely followed by the Anderson-Darling test, and that the Lilliefors test always outperformed the least powerful Kolmogorov-Smirnov test. However, none of these

tests perform well for small sample sizes of fewer than 30 cases [Razali and Wah, 2011], which is the smallest number of years of record required for a catchment to be included in the present study. Because the Shapiro-Wilk, Anderson-Darling and Cramér-von Mises tests gave nearly identical results in this study (and the Kolmogorov-Smirnov test accepted nearly all of the fitted three-parameter distributions so that no distinction between them could be made), only results from the Shapiro-Wilk test will be presented. The significance level chosen for this study is 5% (p-value = 0.05 for the Shapiro-Wilk test).

3.6 Visual inspection of fitted distributions

A visual inspection of a selection of the fitted distributions was carried out, mainly to assist in the interpretation of why certain distributions were rejected, but also to investigate if there were any obvious systematic differences in how the distributions fit to the data. For the 1-month precipitation and streamflow aggregations, all the instances for which the p-value from the Shapiro-Wilk test of normality was <0.05 were plotted as histograms, and the curve for the rejected probability density function added. On each plot, a selection of other fitted distributions were plotted for comparison with the rejected one. To look for clear systematic differences, each selection of distributions was plotted regardless of aggregation duration and Shapiro-Wilk p-value, and subjected to a brief visual overview.

3.7 Proportion of the fitted distribution below zero

Probability distributions that are not bounded below at zero may have a proportion of the fitted distribution occurring for sub-zero quantiles, that is, the cumulative probability distribution $F(x=0) > 0$. Precipitation and river flow data, on the other hand, cannot be negative and in the present study $F(x=0)$ should be zero as all the data exceed zero. The magnitudes of $F(x=0)$ for the fitted distributions were therefore assessed.

3.8 Effects of seasonality and catchment characteristics

The effects of seasonality and catchment characteristics on the goodness-of-fit were investigated for two different measures of goodness-of-fit. First, the rejection rate for each distribution was used, which means stratifying the p-values from the Shapiro-Wilk test on

values below and above 0.05 (the significance level). Second, the average p-values from the Shapiro-Wilk test were investigated. Rejection rates were compared for the winter and summer seasons, and for permeable versus impermeable catchments. Seasonal average p-values for each catchment were used in a correlation analysis with different catchment descriptors. Because of the non-normal distribution of some of the catchment descriptors, correlations were estimated using the non-parametric Spearman's rho. Again, a 5% significance level was employed, based on a two-sided test.

The winter season here comprises October to March and the summer season April to September. Only the 1-month aggregation was used for the seasonal analysis, as the longer the aggregation period for the standardized index is, the less clear the distinction between the seasons become.

4. Results

4.1 Goodness-of-fit

The goodness-of-fit of the selected statistical distributions to the standardized precipitation and streamflow data was assessed, and the results are presented in Table 2. The proportion of occurrences for which the normal distribution cannot be rejected at the 5% significance level (p-value = 0.05) by the Shapiro-Wilk test is shown for all four aggregation durations separately, as well as for all the durations lumped together. In all cases, the 12 calendar months and 121 catchments, are lumped together. Table 2 only shows results for distributions with rejection rates less than 15% for SPI and 20% for SSI, and the remainder of the paper will concern only these distributions. Of the two-parameter distributions, only the Gamma is included in the table. This means that the only distributions with a lower bound at zero that remain in the study are the Gamma, the Tweedie and the three-parameter Kappa distributions. All the unbounded three- and four-parameter distributions are retained. Overall, the rejection rates are higher for the streamflow than for the precipitation data. This seems reasonable since streamflow is affected by the natural and human-induced state of the catchment, e.g. soil moisture content and ground water levels, which can lead to highly variable and non-linear responses to the, in comparison, more regularly-behaving precipitation data.

In the past, the Gamma distribution was often used when calculating the SPI [e.g. *McKee et al.*, 1993; *Lloyd-Hughes and Saunders*, 2002; *Stagge et al.*, 2015] because it has a lower

bound at zero, which agrees with the observed distribution. Others [e.g. *Guttman*, 1999] have argued that three-parameter distributions such as the Pearson type 3 provide a better fit. Although the Gamma distribution has a positive skewness, which generally reflects the behavior of the observed data, distributions with separate location, scale and skewness parameters are more flexible. Table 2 shows that the Gamma distribution is rejected considerably more frequently than any of the three- or four-parameter distributions for both precipitation (9.9%) and streamflow (19.2%).

For both the SPI and the SSI, the distributions rejected the fewest times are the four-parameter and three-parameter Kappa distributions. For the SPI, the Pearson type 3 has the same rejection rate as the three-parameter Kappa distribution, at 1.2% of cases. The Pearson type 3 and the Kappa distributions perform consistently well across all the different durations (Table 2), whereas the rejection rates vary for the other distributions. The Gamma, Generalized Logistic and the two Kappa distributions tend to be rejected less frequently for longer durations than shorter, for both SPI and SSI (Table 2), but the variation with duration is not necessarily monotonic and some distributions seem to fit best for the intermediate durations.

For streamflow, the one month aggregation period is likely to be more useful for drought characterization than it is for precipitation, as there is already a degree of aggregation inherent in streamflow time series, primarily resulting from catchment storage (e.g. *Chiverton et al.*, 2015). For the 1-month SSI, the Gamma distribution is rejected for 29.5% of the cases, whereas the four-parameter Kappa and the Tweedie show the best fits with rejection rates of 3.1% and 5.2%, respectively (Table 2).

4.2 Visual inspection of the fitted distributions

Histograms of the data and fitted distributions were plotted and visually inspected. Two different sets of comparisons are presented for the 1-month aggregations. Figures 2a-c and 3a-c) show examples of the comparison of the fitted Tweedie and Kappa distributions. Figures 2d-f and 3d-f show examples of the comparison between the Gamma, the Tweedie and the best-fitting (according to the Shapiro-Wilk test) of the remaining three-parameter distributions for the SPI and SSI, respectively. The Gamma was included because of its traditional use for the SPI, and the Tweedie because it too is bounded below at zero. This meant the Gamma, Tweedie and Pearson type 3 distributions were compared with each other

for the precipitation data (Figures 2d-f), and the Gamma, Tweedie, Generalized Logistic (better than the GEV overall) and GEV (better than the Generalized Logistic for the 1-month aggregation) distributions were compared for the streamflow data (examples are shown in Figures 3d-f). Table S1 summarizes the overall findings of the present study for these distributions.

With the exception of the very flexible Kappa distributions, the tested theoretical distributions generally struggle to fit bimodal or multimodal data (Figures 2 and 3). However, for non-trivial proportions of cases, both the three- and four-parameter Kappa distributions show signs of over-fitting, resulting in sharp drops/rises and/or sharp bounds at the lower and/or upper ends of the distribution, as well as the peak of the probability density function occurring in unexpected locations (Figures 2a-c and 3a-c). In addition, the four-parameter Kappa distribution does not necessarily encompass all the observed data within its lower and upper bounds (Figures 2a, 2c and 3a), although this occurs also for other distributions such as the GEV (Figure 3f). The effect on the SPI and SSI of observed data occurring outside the bounds will be that the index value becomes undefined (or infinite). The fitted distribution dropping/rising sharply at the tails means that the magnitudes of droughts (or wet periods) will not be well distinguished by the SPI and SSI. The Kappa distributions generally provide a better fit than the Tweedie distribution, as measured by the Shapiro-Wilk p-value (Table 2, Figure 4). However, from an SPI and SSI application perspective, the Tweedie characterizes the tails of the distributions better (Figures 2a-c and 3a-c).

The two-parameter Gamma distribution often gets rejected for bimodal and multimodal data, whereas most of the time the “traditional” three-parameter distributions, although struggling, are accepted (e.g. Figures 2d and 3d). These more flexible distributions tend to fit a reasonably symmetric probability density function, with the Tweedie distribution fitting a somewhat more (positively) skewed curve than the Generalized Logistic, GEV and Pearson type 3 distributions. This “inbetween” behavior explains why the fit of the accepted Tweedie distributions is often slightly worse than that of the more commonly used three-parameter distributions. This can be seen in the generally lower average of the p-values from the Shapiro-Wilk test for the Tweedie distribution compared with the other distributions (Figure 4). For precipitation data, the instances for which the Gamma and Tweedie distributions are not accepted typically coincides with the fitted Pearson type 3 curve having a slight or pronounced negative skewness (similar to Figure 2d). For streamflow, the typical situation

where the Gamma and Tweedie are rejected is for very peaked, positively skewed data, particularly for cases with one or more very extreme values (e.g. Figure 3e). The less flexible fit of the Gamma distribution also sometimes leads to the lower tail not describing the data well (Figure 2f).

In about half of the cases where the Pearson type 3 distributions are not accepted for the 1-month precipitation data, a sharply peaked curve with a very positive skewness has been fitted (e.g. Figure 2b). The fits of the Tweedie and Gamma distributions tend to be both less peaked and less skewed in these cases, and are generally accepted. A closer investigation of the rejected Pearson type 3 occurrences suggests that, particularly for bimodal and multimodal data, the maximum likelihood method has converged on sets of sub-optimal parameter values, as the curves plotted using parameter values based on L-moments provide a (generally accepted) fit more similar to the Tweedie and Gamma distributions. For the Generalized Logistic and GEV fitted to 1-month streamflow data, the distributions fitted using L-moments also often differ substantially to those fitted using maximum likelihood. However, in these cases the data often have a single peak combined with extreme outliers (similar to Figure 3e) and the generally less peaked density curves based on the L-moments do not on the whole provide a better fit as measured by the p-value from the Shapiro-Wilk test.

In very nearly all the cases where the Generalized Logistic distribution fitted to streamflow data is rejected, the fitted density curve is more peaked than for the GEV, Tweedie and Gamma distributions. In about a third of the cases the distribution of the observed data is *very* peaked, similar to Figure 3e. However, in the example in Figure 3e the fitted Generalized Logistic distribution is accepted, and in fact, the Generalized Logistic seems to cope well with very peaked data compared with these other distributions, particularly when also very extreme values are present in the dataset (e.g. Figures 3e-f). The Gamma distribution copes particularly poorly with very extreme values.

Apart from the above mentioned general difficulties in fitting distributions to very peaked or multi-peaked data, or to series that contain very extreme values, it is difficult to find any particular patterns for the rejected GEV distributions. However, the GEV is so flexible that the fitted distributions not infrequently have an abrupt upper bound when fitted to negatively skewed data (Figure 3f). Correspondingly, there is a problem when the fitted distribution has a lower bound greater than zero, which can occur for the four-parameter Kappa (Figures 2a-c

and 3a), the Generalized Logistic (Figure 3e), the Pearson type 3 (Figures 2e-f), as well as for the GEV (Figure 3e and 5b).

Abrupt upper bounds, as well as lower bounds greater than zero, can be avoided altogether by using the Tweedie distribution, which similarly to the Gamma and three-parameter Kappa distribution is bounded below at zero but not above. However, as discussed above, the Tweedie allows for more flexibility in the skewness compared with the Gamma. Table 2 shows that the fit of the Tweedie is second only to the four-parameter Kappa distribution for 1-month streamflow, and is very nearly as good as the Generalized Logistic for all the aggregation durations lumped together (but both are outperformed by the two Kappa distributions). When lumping all the durations together for precipitation, the Tweedie is outperformed by all but the Gamma and GEV distributions, despite having a very low rejection rate at 2.4%.

4.3 Behavior at the lower tail

Figures 2e, 3b and 3e show how the fitted Pearson type 3, Generalized Logistic, GEV and four-parameter Kappa distributions can have part of their mass for quantiles below zero (i.e. $F(0) > 0$), whereas neither precipitation totals or streamflows can be negative. Observed data could be zero, but in the present study all the data are above zero.

The Tweedie distribution is bounded below, but in contrast to the Gamma and three-parameter Kappa distributions, both of which have zero probability for zero precipitation/streamflow, certain parameter values of the Tweedie distribution lead to a positive mass at zero. This means that potentially, if the fit is such that $F(0) \gg 0$, then the same problem would occur as for the distributions that are not bounded below at zero. That is, there would be a lower limit to the SPIs and SSIs. However, for the catchments in the present study, the fitted Tweedie distributions reflect the observed data well and do not have much mass at zero. As can be seen from Table 3, the vast majority of cases has $F(0) < 0.01$, corresponding to an SPI/SSI of -2.33.

Some of the other distributions can also be considered to have acceptably low proportions of $F(0)$, particularly for precipitation. For example, the Pearson type 3 has $F(0) \leq 0.03$ (corresponding to an SPI of -1.88) for all but one out of in total 5808 cases. For streamflow, the values of $F(0)$ are slightly larger.

Figure 5 shows how the fit of the density curve at the lower tail can affect the estimated SPI and SSI during a drought. The 1976 drought was long and severe in the southeast of the UK. Figure 5 shows example histograms and fitted distributions for the Tove at Cappenham Bridge (hydrometric number 33018). For streamflow, the Gamma distribution fits particularly poorly to the data at the lower tail, and data never reach into the lower tail of the distribution. This leads to underestimation of the drought, in the same way as when three-parameter distributions have part of their mass for quantiles less than zero, i.e. $F(0) > 0$ (Figures 5b and 5e). The fitted GEV has a lower bound, leading to an overestimation of drought severity (Figures 5b and 5e). The smallest flow observation is below the lower bound of the GEV, and the SSI 1 – which therefore originally was estimated at minus infinity – was capped at a value of -5.

For precipitation, the fitted probability density curves added to the histograms of the observed 6-month aggregation show no obvious visual differences (Figure 5a), but the time series plots reveal how the different distributions' behaviors at the lower tail affect the SPI 1 and SPI 6 estimates of severe droughts (Figures 5c and 5d).

The SPI 6 time series shows a similar drought progression as the SSI 1 during 1975 and 1976, suggesting that a 6-month aggregation of precipitation reflects the storage in the catchment. However, note that streamflow (SSI 1) in this particular catchment also responds to heavy 1-month precipitation (SPI 1) occurrences not seen in the longer SPI 6 aggregation. This reflects the non-linear relationship between precipitation and runoff, and supports the need for a separate drought index for streamflow. The geology of the Tove catchment is predominantly Chalk, but with 50% overlain by Boulder Clay, a low-permeability superficial deposit. This accounts for the slow response (storage of water in the permeable Chalk aquifer) as well as the fast response (fast runoff from the impermeable areas overlain by clay).

4.4 Effect of seasonality and catchment characteristics on goodness-of-fit

For 1-month precipitation, all distributions except the four-parameter Kappa had smaller rejection rates for winter than for summer, but the differences between the seasons were small. In absolute terms, all the differences were smaller than 1.2 percentage units, except for the Gamma which had a 2.5 percentage unit difference. For 1-month streamflow, all the distributions had smaller rejection rates for winter than for summer. The differences were

527 smaller than 4.4 percentage units for all the distributions, except for the Gamma and the
528 Pearson type 3, which had 22.9 and 28.9 percentage unit difference, respectively.

529 For all the distributions except the Gamma, the absolute difference in rejection rate (lumping
530 all the aggregation durations together) between streamflow in permeable and impermeable
531 catchments was 1.6 percentage units or less, with no consistent variation in the direction of
532 change. For the Gamma distribution, the difference was 6.8 percentage units, with fewer
533 rejections for the impermeable catchments. When only the 1-month aggregation is
534 considered, the differences become slightly larger but still vary in the direction of change.
535 The absolute differences are smaller than 4.0 percentage units, except for the Gamma
536 distribution for which the difference is 13.9 percentage units with fewer rejections in
537 impermeable catchments.

538 Figure 6 shows the seasonal average p-value from the Shapiro-Wilk test for 1-month
539 streamflow in each catchment, for the same selection of distributions as used for the visual
540 inspection in section 4.2. In Figure 6, each dot represents the average of six p-values
541 (averages over April – September for summer, and over October – March for winter). The
542 Gamma distribution is the only distribution for which the average p-values are smaller than
543 0.05 – the statistical significance level for rejection – and these low values all occur in
544 summer. The other distributions also tend to have lower, and spatially more variable, average
545 p-values in summer than in winter, echoing the findings above that rejection rates are higher
546 in summer than in winter. However, the fact that the average p-values are generally much
547 greater than 0.05 suggests that when one of the better-fitting distributions is rejected it tends
548 to be an isolated occurrence, rather than reflecting a larger-scale failure over several months
549 in the same season. The corresponding maps for the 1-month precipitation analysis did not
550 reveal any obvious seasonal or geographical differences in the goodness-of-fits (not shown).

551 Correlations between seasonal average p-values and catchment descriptors are shown in
552 Table 4. There is little evidence of catchment characteristics (AREA and SAAR) influencing
553 the goodness-of-fit of the 1-month precipitation data, particularly in winter, as most
554 distributions fit these data well. For 1-month streamflow, the majority of the correlations are
555 rather weak and not significant at the 5% level, although a couple of correlations each for the
556 Gamma and GEV distributions exceed 0.4. Broadly, correlations are often positive (but not
557 necessarily significant) for SAAR and AREA, and negative for SMDBAR. Correlations with

BFIHOST are also mostly negative, but with notable exceptions for the Generalized Logistic and GEV distributions in summer.

4.5 Influence of season and duration on the Tweedie parameter ξ

As mentioned in the methods section, the Tweedie is a family of distributions whose special cases include the Normal ($\xi = 0$), Poisson ($\xi = 1$), Gamma ($\xi = 2$), and Inverse Gaussian ($\xi = 3$) distributions [e.g. *Tweedie*, 1981; *Dunn and Smyth*, 2005]. The value of the parameter ξ is constrained in the estimation procedure to be at least 1.2 (see Appendix B for further details), which means that the estimated Tweedie distribution will never correspond to a Normal or a Poisson distribution. However, in the height of winter (January) the ξ values tend to approach 1 from above for both 1-month precipitation and 1-month streamflow (not shown), in response to the distributions being rather symmetric. In contrast, more positively skewed distributions in the height of summer (July), lead to ξ values being clustered between 2 and 3, i.e. suggesting distributions more similar to the Gamma and Inverse Gaussian. Most of the time ξ values do not go far above 3 for 1-month precipitation, whereas for 1-month streamflow in the summer half-year they are not unusual up to 5 and may go as high as 7. Distributions tend to become more symmetric with increasing aggregation duration, and the longer the duration the more the ξ values tend to approach 1 from above.

5. Discussion

Following the general acceptance of the SPI as a tool for drought monitoring, there has been a growing interest in the application of standardization methods to other variables such as streamflow. Time series of drought indices like the SPI and SSI require a statistical distribution function to be fitted to the observed (generally monthly) precipitation and streamflow data. Previous research has underlined the challenges associated with finding appropriate probability distributions for these purposes, and there is generally limited consensus on which to choose, which highlights the importance of testing distributions in the region of interest. For example, *Stagge et al.* [2015] tested a range of distributions for the SPI, using gridded precipitation data across Europe. Although they concluded that the Gamma distribution generally showed a good fit for aggregations longer than one month, the UK was one of the regions for which rejection rates were high. The present paper uses

observed streamflows and catchment average rainfalls from a diverse set of catchments in the UK. It extends the SPI study of *Stagge et al.* [2015] by also investigating the Generalized Logistic, Pearson type 3, GEV, Tweedie and four-parameter Kappa distribution, as well as versions of the Generalized Logistic and Kappa distributions constrained to have a lower bound at zero (making them two- and three-parameter distributions, respectively). In addition, the inclusion of distributions that do not necessarily have a lower bound meant we also investigated how many of the fitted distributions have a significant proportion of their mass below zero.

Longer aggregations of data tend to have a more symmetric shape of the distribution than shorter aggregations, which often have a positive skewness. Different distributions therefore fit the data with varying success, and the practitioner could apply different distributions to different aggregation durations and types of data. The ideal statistical distribution would be bounded below by zero, but would have enough flexibility to fit the full range of behaviors exhibited by the observed data for UK conditions. The Shapiro-Wilk test for goodness-of-fit would suggest that the three-parameter Kappa distribution fulfils these expectations. However, both the three- and four-parameter Kappa distributions were found to over-fit the data, and to include fitted probability density functions with abrupt drops/rises and, in the case of the four-parameter Kappa, sharp bounds at its lower and upper tails (Figures 2a-c and 3a-c). Such behavior at the tails is highly detrimental for accurately discerning the severity of extreme droughts (or periods of wetness) as measured by the SPI or SSI. Further, when the peak of the probability density function is displaced (often resulting in a negative skewness, as in Figures 2a-c and 3c), this also results in a bias in the general characterization of dry versus wet conditions. Typically, conditions that should be considered wet are labelled dry.

The over-fitting is a result of the Kappa distribution being very flexible, and the sample sizes being rather small and the data exhibiting bi- or multimodality. While increased sample sizes can be expected with time, at present it may be better to use a less flexible distribution like the Tweedie. Future work on the three-parameter Kappa distribution could include investigating the parameter values that lead to sharp drops at the tails of the probability density function and then, if possible, constraining the parameter space accordingly when fitting the distribution.

Of the options investigated in the present study, the Tweedie family of distributions largely meets the criteria of a sensible and reasonably flexible fit combined with a lower bound at

zero. It can therefore be expected that future applications of SPI and SSI in the UK would benefit from employing this distribution. Given the suitability of the Tweedie distribution across a wide range of catchment types, it is likely that it will perform well also in other settings. Given the previous lack of suitability of any one parametric method in past SSI applications [Vicente Serrano *et al.*, 2012; Soláková *et al.*, 2014], we recommend further research to examine the suitability of the Tweedie distribution in other environments. Its general suitability for both SPI and SSI suggests it could also be applied to standardized indicators used for other compartments of the hydrological cycle. The fact that the Tweedie distribution can have positive mass at zero makes it particularly suitable for arid and semi-arid climates and for ephemeral streams, which is desirable given the acknowledged issues associated with application of the SPI in arid locations [Wu *et al.*, 2007].

Despite its clear potential, there are practical drawbacks associated with the Tweedie distribution. Only for a small number of special cases can the distributions be written in closed form. Numerical methods therefore need to be used, making distribution fitting time consuming. Thus, while the Tweedie family is the most suitable choice when computational resources allow, for some applications it may be less desirable than conventional distributions. For example, for large gridded datasets, computer time requirements are likely to be high. However, this does not preclude its use, as once distribution parameters are derived, future applications (e.g. in updating a monitoring and early warning system on a monthly basis using parameters already estimated for a fixed reference period) would be no more computationally demanding than for other distributions.

This study has also provided valuable information on the applications of other distribution functions. Although not ideal, for the catchments and aggregation durations used in the present study, the proportions of the fitted theoretical distributions falling below zero may be acceptably small for some of the best-fitting three-parameter distributions: the Pearson type 3 (for precipitation), and the GEV and Generalized Logistic (for streamflow) distributions.

When investigating statistical distributions suitable for the standardized precipitation evapotranspiration index (SPEI), Vicente-Serrano *et al.* [2010] found that goodness-of-fit tests struggled to distinguish between candidate distributions. Instead, they made the final selection based on the behavior of the tails of the distributions. They found that the thicker tail of the Generalized Logistic (termed Log-logistic in their paper) could more easily accommodate the extremes of the lower tail, than could the Pearson type 3, the Lognormal

and the GEV distributions. *Vicente-Serrano and Beguería* [2015] investigated the difference between the GEV and the Generalized Logistic in even more detail regarding goodness-of-fit, behavior at the tails of the distribution, and fraction of cases with no solution, and reaffirmed their preference for the Generalized Logistic. However, *Stagge et al.* [2016] subsequently argued that the GEV models the extreme tails better and that the Generalized Logistic consistently underestimate these values, although they conclude that there is significant uncertainty due to extrapolation regardless of distribution. Considering the subjectivity of the visual inspection in the present study and the limited sample sizes used for the goodness-of-fit tests, we will not argue either way from a goodness-of-fit perspective of the extreme tail. However, a thicker tail like that of the Generalized Logistic distribution is an advantage when parameters have been estimated for a fixed reference period, and the same distribution parameters are later used when updating the series [compare *Tanguy et al.*, 2015]. The reference period may not have included very extreme values, and a thick-tailed distribution makes it less likely that an unprecedentedly large future observation results in a standardized index that is undefined or equal to infinity. In this context it is also worth mentioning that an imposed lower bound needs to be at zero, rather than above (or below) zero. A lower bound above zero will result in calculated standardized climate indices that are either undefined or equal to negative infinity for observations that fall below the lower bound. Note that using a fixed reference period assumes that data is stationary, and the distribution parameters would need to be re-assessed to take into account the effect of climate, or other environmental, change.

The rejection rates for the distributions tended to be greater in summer than in winter for both precipitation and streamflow, although the differences were generally rather small for distributions that fitted the data well. For both variables, the seasonal differences presumably reflect the more erratic behavior of convective activity in summer, and the more regular behavior of frontal precipitation in winter. For streamflow, soil moisture deficits are also more variable in summer than in winter, leading to a less regular runoff response. These results can be compared with those of *Stagge et al.* [2015], who found no seasonal differences in rejection rates for Weibull distributions fitted to 1-month gridded precipitation data across Europe.

Rather than stratifying on overall rejection/acceptance rates, using the seasonal average p-value from the Shapiro-Wilk test for individual catchments makes possible a spatial evaluation based on a more nuanced measure of goodness-of-fit. For streamflow (Figure 6),

the most spatially and seasonally consistent (least variable) p-values are those for the Tweedie and unconstrained Kappa distributions, although for summer both struggle with an area of small, and predominantly very permeable, catchments in the southeast. Permeable catchments with a large groundwater contribution to flows exhibit persistence of wet and dry spells that can last several years [e.g. *Wilby et al.*, 2015]. This can lead to clusters of high and/or low values in the record (and thus bi- or multi-modal empirical distributions), making statistical distribution-fitting difficult. Compared with the northwest, the southeast has a comparatively continental climate: evaporation is larger, which leads to higher soil moisture deficits and potentially erratic flow responses, particularly in permeable catchments. Also, although average rainfall is lower, heavy convective rainfalls in summer are more common. For small catchments, this means that localized convective rainfalls can have a greater impact on the streamflow than it would in larger catchments. The correlation analysis between summer average p-values and catchment characteristics supports the above reasoning in so far as to the sign of the correlations, and the pattern can largely be generalized to most of the distributions, and to winter. However, statistically significant relationships are few and mainly occur for the poorer-fitting distributions.

6. Conclusions

Drought indicators can be used as triggers for action and declaration of drought, and form the foundation of drought monitoring and early warning. Standardized indices such as the SPI (for precipitation) and SSI (for streamflow) allow fair comparison between different locations and different seasons. They are also flexible in that they can be aggregated across a range of timescales (e.g. 1, 3, 6, 12 months), which are relevant for different types of drought impacts. The derivation of the SPI and SSI require a statistical distribution to be fitted to the observed data. Here, we have presented a study of the goodness-of-fit and tail behavior of twelve different distributions for a diverse set of 121 catchments in the UK, as well as the influence of seasonality and catchment characteristics on these fits.

Both precipitation and streamflow data are bounded below at zero, as precipitation and flows cannot be negative. Their empirical distributions also tend to have positive skewness, and therefore the Gamma distribution has often been a natural and suitable choice for describing the data statistically [e.g. *Stagge et al.*, 2015]. However, after transformation of the data to

Normal distributions to obtain the SPIs and SSIs for the UK catchments, the distributions are rejected in 9.9% and 19.2% of cases, respectively, by the Shapiro-Wilk test.

The best fitting distributions are the three- and four-parameter Kappa distributions (the former being a version of the latter with a lower bound at zero imposed). However, both were seen to over-fit to the data, resulting in sharp drops and rises of the probability density function near the tails, making it difficult to accurately discern the severity of extreme droughts (or periods of wetness) from the calculated SPI and SSI.

Other three-parameter distributions traditionally used in hydrological applications, such as the Pearson type 3 for precipitation and the Generalized Logistic and GEV distributions for streamflow, fit the transformed data reasonably well, with rejection rates of 5% or less. However, in most cases these three-parameter distributions do not have a lower bound at zero. This means that the lower tail of the fitted distribution may potentially go below zero, which would result in a lower limit to the calculated SPI and SSI values (as observations can never reach into this lower tail of the theoretical distribution). In contrast, the Tweedie distribution is a flexible three-parameter distribution that has a lower bound at zero. It fits both precipitation and streamflow data nearly as well as the best of the traditionally used three-parameter distributions, with rejection rates of 2.4% and 3.9% for precipitation and streamflow, respectively. The Tweedie distribution has only recently been applied to precipitation data, and only for a few sites. As far as the authors are aware, it has never been applied to streamflow data. The Tweedie probability density function can only be written in closed form for a few special cases, which means that parameter estimation is time consuming. However, recent advances in parameter estimation methods, and implementation of these methods in the R package “tweedie” [Dunn, 2015], mean that the use of the Tweedie distribution is now a viable option. The Tweedie distribution thus has significant potential for use in future drought indicator applications in the UK, and has properties which make it well suited for use in other environments. Particularly, its possibility of having mass at zero makes it a proposition for drier climates. A further advantage is its encompassing of several other distributions as special cases, which allows a greater flexibility in the possible shapes of the distribution without having to make an a priori distributional choice. More generally, the Tweedie could have utility for a range of other hydrological applications, suggesting further research is needed to explore its full potential.

This study also investigated the effect of seasonality and catchment characteristics on the goodness-of-fit of the statistical distributions. For both precipitation and streamflow data, most distributions were found to have larger rejection rates in summer than in winter, although for well-fitting distributions the differences were rather small. Similarly, catchment characteristics generally had little impact on the suitability of a distribution.

Acknowledgments

This study is an outcome of the Belmont Forum project DrIVER (Drought Impacts: Vulnerability thresholds in monitoring and Early warning Research). Financial support for C. Svensson and J. Hannaford within the DrIVER project was provided by the UK Natural Environment Research Council (Grant NE/L010038/1). Financial support for I. Prosdocimi was provided by NERC/CEH National Capability funding. The use of daily mean streamflow data, catchment average monthly precipitation data, and catchment descriptors provided by the National River Flow Archive (NRFA) is gratefully acknowledged. The data used in this study can be obtained free of charge from the NRFA website (<http://nrfa.ceh.ac.uk/>).

References

- Bachmair, S., K. Stahl, K. Collins, J. Hannaford, M. Acreman, M. Svoboda, C. Knutson, K. Helm Smith, N. Wall, B. Fuchs, N. D. Crossman, and I. C. Overton (2016), Drought indicators revisited: the need for a wider consideration of environment and society, *Wiley Interdisciplinary Reviews: Water* 3(4), 516-536, doi: 10.1002/wat2.1154.
- Barker, L. J., J. Hannaford, A. Chiverton, and C. Svensson (2016), From meteorological to hydrological drought using standardised indicators, *Hydrol. Earth Syst. Sci.*, 20, 2483-2505, doi: 10.5194/hess-20-2483-2016.
- Bayliss, A. (1999), Flood Estimation Handbook vol. 5: Catchment descriptors, Institute of Hydrology, Wallingford, UK.
- Bloomfield, J. P., and B. P. Marchant (2013), Analysis of groundwater drought building on the standardised precipitation index approach, *Hydrol. Earth Syst. Sci.*, 17(12), 4769-4787, doi:10.5194/hess-17-4769-2013.
- Bradford, R. B., and T. J. Marsh (2003), Defining a network of benchmark catchments for the UK, *P. I. Civil Eng. – Water & Mar. En.*, 156(WM2), 109-116.
- Chiverton, A., J. Hannaford, I. Holman, R. Corstanje, C. Prudhomme, J. Bloomfield, and T. M. Hess (2015), Which catchment characteristics control the temporal dependence structure of daily river flows? *Hydrol. Process.*, 29(6), 1353-1369, doi: 10.1002/hyp.10252.
- Collins, K., J. Hannaford, S. Haines, L. Stephens (2015), Drought: understanding and reducing vulnerability through monitoring and early warning systems. Report of the DrIVER workshop, 17 March 2015, Wallingford, UK.
- Dunn, P. K. (2004), Occurrence and quantity of precipitation can be modelled simultaneously, *Int. J. Climatol.*, 24(10), 1231-1239, doi: 10.1002/joc.1063.
- Dunn, P. K. (2015), Package ‘tweedie’. Description of the R programming language package ‘tweedie’, <http://cran.r-project.org/web/packages/tweedie/tweedie.pdf> (link accessed on 14 September 2016).
- Dunn, P. K. and G. K. Smyth (2001), Tweedie family densities: methods of evaluation, Proc. 16th International Workshop on Statistical Modelling, Odense, Denmark, 2-6 July 2001, 8 pp.

793 Dunn, P. K. and G. K. Smyth (2005), Series evaluation of Tweedie exponential dispersion
794 model densities, *Stat. Comput.*, 15(4), 267-280, doi: 10.1007/s11222-005-4070-y.

795 Dunn, P. K. and G. K. Smyth (2008), Evaluation of Tweedie exponential dispersion model
796 densities by Fourier inversion, *Stat. Comput.*, 18(1), 73-86, doi: 10.1007/s11222-007-9039-6.

797 Farrell, P. J. and K. Rogers-Stewart (2006), Comprehensive study of tests for normality and
798 symmetry: extending the Spiegelhalter test. *J. Stat. Comput. Sim.*, 76(9), 803-816, doi:
799 10.1080/10629360500109023.

800 Folland, C. K., J. Hannaford, J. P. Bloomfield, M. Kendon, C. Svensson, B. P. Marchant, J.
801 Prior, and E. Wallace (2015), Multi-annual droughts in the English Lowlands: a review of
802 their characteristics and climate drivers in the winter half-year, *Hydrol. Earth Syst. Sci.*,
803 19(5), 2353-2375, doi: 10.1080/10629360500109023.

804 Gosling, R. (2014), Assessing the impact of projected climate change on drought
805 vulnerability in Scotland, *Hydrol. Res.*, 45(6), 806-816, doi: 10.2166/nh.2014.148.

806 Gudmundsson, L., and J. H. Stagge (2015), Package ‘SCI’. Description of the R
807 programming language package ‘SCI’, <http://cran.r-project.org/web/packages/SCI/SCI.pdf>
808 (link accessed on 14 September 2016).

809 Guttman, N. B. (1999), Accepting the standardized precipitation index: a calculation
810 algorithm. *J. Am. Water Resour. As.*, 35(2), 311-322, doi: 10.1111/j.1752-
811 1688.1999.tb03592.x.

812 Hannaford, J., B. Lloyd-Hughes, C. Keef, S. Parry, and C. Prudhomme (2011), Examining
813 the large-scale spatial coherence of European drought using regional indicators of
814 precipitation and streamflow deficit, *Hydrol. Process.*, 25(7), 1146-1162, doi:
815 10.1002/hyp.7725.

816 Hasan, M. M. and P. K. Dunn (2011), Two Tweedie distributions that are near-optimal for
817 modelling monthly rainfall in Australia. *Int. J. Climatol.*, 31, 1389-1397, doi:
818 10.1002/joc.2162.

819 Hayes, M., M. Svoboda, N. Wall, and M. Widhalm (2011), The Lincoln Declaration on
820 Drought Indices, *B Am Meteorol Soc*, 92(4), 485-488, doi: 10.1175/2010BAMS3103.1.

821 Hosking, J. R. M. (2015), Package ‘lmom’. Description of the R programming language
 822 package ‘lmom’, <https://cran.r-project.org/web/packages/lmom/lmom.pdf> (link accessed on
 823 14 September 2016.

824 Hosking, J. R. M., and J. R. Wallis (1997) Regional frequency analysis – An approach based
 825 on L-moments, Cambridge University Press, Cambridge, UK.

826 Jørgensen, B. (1987), Exponential dispersion models, *J. R. Statist. Soc. B*, 49(2), 127-162.

827 Jørgensen, B., and M. C. Paes de Souza (1994), Fitting Tweedie's compound Poisson model
 828 to insurance claims data, *Scand. Actuar. J.*, 1994(1), 69-93, doi:
 829 10.1080/03461238.1994.10413930.

830 Lloyd-Hughes, B. (2014), The impracticality of a universal drought definition, *Theor. Appl.*
 831 *Climatol.*, 117(3-4), 607-611, doi: 10.1007/s00704-013-1025-7.

832 Lloyd-Hughes, B. and M. A. Saunders (2002), A drought climatology for Europe, *Int. J.*
 833 *Climatol.*, 22(13), 1571-1592, doi: 10.1002/joc.846.

834 Lorance, P., L. Pawlowski, and V. M. Trenkel (2010), Standardizing blue ling landings per
 835 unit effort from industry haul-by-haul data using generalized additive models, *ICES J. Mar.*
 836 *Sci.*, 67(8), 1650-1658, doi: 10.1093/icesjms/fsq048.

837 Marsh, T. J. and J. Hannaford (Eds.) (2008), UK Hydrometric Register. Hydrological data
 838 UK series, Centre for Ecology & Hydrology, Wallingford, UK, 210 pp.

839 McKee, T. B., N. J. Doelsken and J. Kleist (1993), The relationship of drought frequency and
 840 duration to time scales. Proc. Eighth Conference on Applied Climatology, 17-22 January
 841 1993, Anaheim, California, 6 pp.

842 Núñez, J., D. Rivera, R. Oyarzún, and J. L. Arumí (2014), On the use of Standardized
 843 Drought Indices under decadal climate variability: Critical assessment and drought policy
 844 implications, *J. Hydrol.*, 517, 458-470, doi: 10.1016/j.jhydrol.2014.05.038.

845 Razali, N. M. and Y. B. Wah (2011), Power comparisons of Shapiro-Wilk, Komogorov-
 846 Smirnov, Lilliefors and Anderson-Darling tests, *Journal of Statistical Modeling and*
 847 *Analysis*, 2(1), 21-33.

848 Shukla, S., and A. W. Wood (2008), Use of a standardized runoff index for characterizing
 849 hydrologic drought, *Geophys. Res. Lett.*, 35(2), L02405, doi: 10.1029/2007GL032487.

850 Sienz, F., O. Bothe, and K. Fraedrich (2012), Monitoring and quantifying future climate
851 projections of dryness and wetness extremes: SPI bias, *Hydrol. Earth Syst. Sci.*, 16(7), 2143-
852 2157, doi:10.5194/hess-16-2143-2012.

853 Soláková, T., C. De Michele, and R. Vezzoli (2014), Comparison between Parametric and
854 Nonparametric Approaches for the Calculation of Two Drought Indices: SPI and SSI, *J.*
855 *Hydrol. Eng.*, 19(9), 04014010, doi: 10.1061/(ASCE)HE.1943-5584.0000942.

856 Stagge, J. H., L. M. Tallaksen, L. Gudmundsson, A. F. van Loon, and K. Stahl (2015),
857 Candidate distributions for climatological drought indices (SPI and SPEI), *Int. J. Climatol.*,
858 35(13), 4027-4040, doi: 10.1002/joc.4267.

859 Stagge, J. H., L. M. Tallaksen, L. Gudmundsson, A. F. van Loon, and K. Stahl (2016),
860 Response to comment on ‘Candidate distributions for climatological drought indices (SPI and
861 SPEI)’, *Int. J. Climatol.*, 36(4), 2132-2138, doi: 10.1002/joc.4564.

862 Staudinger, M., K. Stahl, and J. Seibert (2014), A drought index accounting for snow, *Water*
863 *Resour. Res.*, 50(10), 7861-7872, doi: 10.1002/2013WR015143.

864 Tanguy, M., J. Hannaford, L. Barker, C. Svensson, F. Kral, and M Fry (2015) Gridded
865 Standardised Precipitation-Evapotranspiration Index (SPEI) using generalised logistic
866 distribution with standard period 1961-2010 for Great Britain [SPEIgenlog61-10]
867 doi:10.5285/d201a2af-568e-4195-bf02-961fb6954c72 – Supporting Information for dataset,
868 NERC Environmental Information Data Centre, UK, 8 pp.

869 Tweedie, M. C. K. (1981), An index which distinguishes between some important
870 exponential families. In *Statistics: Applications and New Directions*, Proceedings of the
871 Indian Statistical Institute Golden Jubilee International Conference, edited by Ghosh, J. K.
872 and Roy, J., pp. 579-604, Indian Statistical Institute, Calcutta, India.

873 Vicente-Serrano, S. M., and S. Beguería (2015), Comment on ‘Candidate distributions for
874 climatological drought indices (SPI and SPEI)’ by James H. Stagge *et al.*, *Int. J. Climatol.*,
875 36(4), 2120-2131, doi: 10.1002/joc.4474.

876 Vicente-Serrano, S. M., S. Beguería, and J. I. López-Moreno (2010), A Multiscalar Drought
877 Index Sensitive to Global Warming: The Standardized Precipitation Evapotranspiration
878 Index, *J. Climate*, 23(7), 1696-1718, doi: 10.1175/2009JCLI2909.1.

- Vicente-Serrano, S. M., J. I. López-Moreno, S. Beguería, J. Lorenzo-Lacruz, C. Azorin-Molina, and E. Morán-Tejeda (2012), Accurate Computation of a Streamflow Drought Index, *J. Hydrol. Eng.*, 17(2), 318-332, doi: 10.1061/(ASCE)HE.1943-5584.0000433.
- Wilby, R. L., C. Prudhomme, S. Parry, and K. G. L. Muchan (2015), Persistence of hydrometeorological droughts in the United Kingdom: A regional analysis of multi-season rainfall and river flow anomalies, *J. Extreme Events*, 2(2), 1550006 (27pp), doi: 10.1142/S2345737615500062.
- Wilhite, D., and M. Glantz (1985), Understanding: the drought phenomenon: the role of definitions, *Water Int.*, 10(3), 111-120, doi:10.1080/02508068508686328.
- Wu, H., M. J. Hayes, D. A. Wilhite, and M. D. Svoboda (2005), The effect of the length of record on the standardized precipitation index calculation, *Int. J. Climatol.*, 25(4), 505-520, doi: 10.1002/joc.1142.
- Wu, H., M. D. Svoboda, M. J. Hayes, D. A. Wilhite, and F. J. Wen (2007), Appropriate application of the Standardized Precipitation Index in and locations and dry seasons, *Int. J. Climatol.*, 27(1), 65-79, doi: 10.1002/joc.1371.

Appendix A. The Tweedie family of distributions

The concept of the Tweedie family of distributions was comprehensively outlined by *Tweedie* [1984], and further explored by *Jørgensen* [1987]. The Tweedie family of distributions is a special class within the so called exponential dispersion models (EDMs). A random variable Y that follows an EDM has a probability density function on the form

$$f(y; \mu, \phi) = a(y, \phi) \exp \left[\frac{1}{\phi} \{y\theta - \kappa(\theta)\} \right],$$

where $\mu = E[Y] = \kappa'(\theta)$ is the mean, $\phi > 0$ is the dispersion parameter, θ is the canonical parameter and $\kappa(\theta)$ is the cumulant function (the latter two are both known). The function $a(y, \phi)$ cannot generally be written in closed form, apart from for some special cases. The variance is given by $\text{var}[Y] = \phi V(\mu)$ where $V(\mu) = \kappa''(\theta)$ is the variance function viewed as a function of the mean μ . The Tweedie family of distributions is a class of EDMs characterized by the variance function $V(\mu)$ having a power relationship to the mean, μ , as $V(\mu) = \mu^\xi$ for $\xi \notin (0, 1)$, where ξ specifies the particular distribution. Special cases include the Normal ($\xi = 0$), Poisson ($\xi = 1$), Gamma ($\xi = 2$), and Inverse Gaussian ($\xi = 3$) distributions [e.g. *Dunn and Smyth*, 2001; *Hasan and Dunn*, 2011]. Apart from for these special cases, numerical methods need to be used for estimating the distribution parameters [e.g. *Dunn and Smyth*, 2001; 2008]. Although time consuming compared with parameter estimation for distributions with explicit analytic forms, the implementation of such methods in the R package ‘tweedie’ [*Dunn*, 2015] means that application of the Tweedie distribution is now a more practicable option.

When the Tweedie parameter ξ has a value between 1 and 2, the distribution describes series that contain exact zeroes as well as positive continuous data. *Dunn* [2004] refers to this particular case as a Poisson-gamma distribution, and explains the underlying assumptions when applying it to precipitation data as follows. If the number of precipitation events occurring within a time period is assumed to have a Poisson distribution, and the magnitude of each event is Gamma distributed, then the total precipitation amount within the time period can be found as the Poisson sum of the Gamma distributed random variables. This distribution has also been referred to as a compound Poisson distribution by, for example, *Jørgensen and Paes de Souza* [1994] who used it to model total insurance claims costs per

925 insured unit (assuming the number of individual claims within the unit to be Poisson
926 distributed and the cost for each individual claim to be Gamma distributed).

927 The EDMs are a generalization of (linear) exponential families, and describe the error
928 distribution of generalized linear models (GLMs) [e.g. *Jørgensen*, 1987]. *Hasan and Dunn*
929 [2011] note that a framework is therefore already in place for fitting GLMs based on the
930 Tweedie distributions, and for diagnostic testing. Further, it is straight-forward to incorporate
931 covariates into the modelling procedure. This has been done by, for example, *Lorance et al.*
932 [2010] for estimating fish landings per unit effort using generalized additive models with
933 explanatory variables such as depth, area and year.

934

935

Appendix B. Fitting statistical distribution functions

A range of two- and three-parameter probability distributions was investigated, as well as one four-parameter distribution: the Kappa distribution. The three-parameter distributions included the Generalized Logistic, Pearson type 3, Generalized Extreme Value (GEV) and Tweedie, as well as the Kappa distribution with a lower bound at zero imposed (which reduces it to a three-parameter distribution). The two-parameter distributions included the Gamma, Lognormal, Normal, Gumbel and Weibull distributions, as well as the Generalized Logistic distribution with a lower bound at zero (which reduces it to a two-parameter distribution). The definitions of the probability density functions are given in *Stagge et al.* [2015], except for the Tweedie which is described by *Dunn and Smyth* [2005] and the Kappa which is described in *Hosking and Wallis* [1997]. The constraints of a lower bound at zero were implemented based on the equations for the lower bounds given in *Hosking and Wallis* [1997]. It can be noted that the distribution that is referred to as the Generalized Logistic in the present paper and in *Stagge et al.* [2015], follow the definition in *Hosking and Wallis* [1997]. Others, for example *Vicente-Serrano et al.* [2010] and *Vicente-Serrano and Beguería* [2015], refer to this same distribution as the Log-logistic distribution.

Computationally, the aggregation of the data into durations longer than a month and the fitting of the distributions to the aggregated series were done using the function `fitSCI` in the R package ‘SCI’ (which calls other packages to do the actual fits) [*Gudmundsson and Stagge*, 2015]. All of the distributions except the Tweedie, the Kappa and the distributions bounded below at zero are available within the ‘SCI’ package. In order to incorporate these latter distributions into the ‘SCI’ framework, new start functions for parameter estimates were written (`start.fun` in the `fitSCI` function). For all distributions except the Tweedie, the starting values for the maximum likelihood estimation of the parameter values were based on L-moments. The initial, complete, set of L-moment-based parameter estimates were obtained according to *Hosking and Wallis* [1997], using the `samlmu`, `pelglo` and `pelkap` functions in the R package ‘lmom’ [*Hosking*, 2015]. For the constrained distributions, these initial parameter estimates were then amended to make the distributions conform to having a lower bound at zero, based on the equations for the lower bounds given in *Hosking and Wallis* [1997]. For the Generalized Logistic distribution, the location and scale parameter estimates were kept, and the shape parameter, k , amended. Similarly, for the Kappa distribution, all L-moment-based parameter estimates except the parameter k were kept, and k was amended.

For the Tweedie distribution, the start function obtained the parameter estimates by calling the function `tweedie.profile` in the R package ‘tweedie’ [Dunn, 2015]. The Tweedie parameters μ (the mean), ξ (the power) and ϕ (the dispersion) are estimated using maximum likelihood as described by Dunn [2015] and Dunn and Smyth [2005], using their suggested order of preference regarding estimation method. When ξ is close to one, the probability density function becomes multimodal, reflecting that at this limit it is a Poisson distribution which is discrete [Dunn and Smyth, 2005]. The value of the parameter ξ was therefore constrained. Dunn [2015] recommends a minimum ξ of 1.2 for data containing zeroes and 1.5 for data without zeroes. The higher limit results in fewer distributions being fitted with mass at zero ($F(0)>0$). However, there is a trade-off with the fit of the distributions, as particularly for longer aggregation durations the distributions become more symmetrical and the optimum value of ξ decreases towards 1. In the present study $\xi \geq 1.2$ has been used as we found the values of $F(0)$ in Table 3 acceptable.

If possible, the parameter values for the distributions available in ‘SCI’ are estimated using maximum likelihood. However, if the maximum likelihood method fails to converge, an attempt is first made to estimate the parameter values using L-moments, and failing that too, the method of moments is used. For the bounded distributions and the four-parameter Kappa distribution, L-moment estimators were used if the maximum likelihood procedure did not converge. For most distributions, the maximum likelihood procedure failed to converge for (much) less than one percent of cases. However, for the GEV and the four-parameter Kappa distribution the failure rates were 2.6% and 3.4% (GEV) and 23% and 40% (Kappa) for precipitation and river flow data, respectively.

Once the distributions had been fitted, the standardized indices were calculated using the function `transformSCI` in the R package ‘SCI’. The function `ptweedie` in the ‘tweedie’ package was amended to cope with i) the SCI function `transformSCI` passing the vector of quantiles to `ptweedie` as mode list rather than numeric, and ii) the vector of quantiles containing missing values.

997 **Tables**

998

999 **Table 1.** Statistical probability distributions investigated. Bold italic font denote distributions with a lower bound at zero. Arrows indicate where
1000 a distribution with fewer parameters is a special case or variant of a more general distribution.

1001

4 parameters (very flexible)	3 parameters (flexible)	2 parameters (less flexible)
	Generalized Logistic	→ <i>Generalised Logistic</i> (lower bound imposed)
	Pearson type 3	→ <i>Gamma</i>
	Generalized Extreme Value	→ { <i>Weibull</i> Gumbel
	<i>Tweedie</i>	(→)* Normal
		<i>Lognormal</i>
Kappa4	→ <i>Kappa3</i> (lower bound imposed)	

1002 * The way the Tweedie distribution is constrained in the present study, it does not include the Normal distribution as an option.

1003

1004

1005 **Table 2.** Percentage of occurrences for which the normal distribution is rejected at the 5% significance level by the Shapiro-Wilk test for SPI
 1006 and SSI of different aggregation durations, and for all durations together. Results are lumped together for the 121 catchments and the 12
 1007 calendar end months. Distributions in bold italic font have a lower bound at zero.

Distribution	All SPI	SPI 1	SPI 3	SPI 6	SPI 12	All SSI	SSI 1	SSI 3	SSI 6	SSI 12
<i>Gamma</i>	<i>9.9</i>	<i>17.5</i>	<i>6.5</i>	<i>7.0</i>	<i>8.6</i>	<i>19.2</i>	<i>29.5</i>	<i>18.9</i>	<i>12.3</i>	<i>16.0</i>
Generalized Logistic	1.8	3.7	1.4	1.6	0.6	3.8	9.0	3.7	1.6	0.9
Pearson type 3	1.2	2.1	0.6	0.9	1.2	10.5	25.9	11.6	3.5	1.0
GEV	3.5	1.2	1.2	3.9	7.6	4.7	6.6	2.8	3.0	6.4
<i>Tweedie</i>	<i>2.4</i>	<i>2.1</i>	<i>0.8</i>	<i>2.0</i>	<i>4.8</i>	<i>3.9</i>	<i>5.2</i>	<i>2.5</i>	<i>2.5</i>	<i>5.4</i>
<i>Kappa3</i>	<i>1.2</i>	<i>1.7</i>	<i>0.9</i>	<i>1.5</i>	<i>0.6</i>	<i>2.2</i>	<i>5.5</i>	<i>1.7</i>	<i>1.0</i>	<i>0.8</i>
Kappa4	0.7	1.2	0.4	0.8	0.5	1.3	3.1	1.3	0.3	0.3

1008

1009

1010

1011 **Table 3.** Counts of $F(0)$ in different magnitude intervals. If $F(0)$ is large, then a large part of the fitted theoretical distribution occurs for data
1012 values at or below zero. Results are lumped for the 121 catchments, the four aggregation durations, and the 12 calendar end months.

Magnitude of $F(0)$	Lower bound of SPI (or SSI) corresponding to $F(0)$	Precipitation					Streamflow				
		Generalized Logistic	Pearson type 3	GEV	Tweedie	Kappa4	Generalized Logistic	Pearson type 3	GEV	Tweedie	Kappa4
$F(0) \leq 0.01$	$SPI \leq -2.33$	5358	5694	5557	5798	5746	5373	5653	5458	5791	5631
$0.01 < F(0) \leq 0.02$	$-2.33 < SPI \leq -2.05$	322	100	216	10	40	255	106	248	17	98
$0.02 < F(0) \leq 0.03$	$-2.05 < SPI \leq -1.88$	104	13	32	0	15	137	14	70	0	53
$0.03 < F(0) \leq 0.04$	$-1.88 < SPI \leq -1.75$	22	1	3	0	6	31	0	20	0	20
$0.04 < F(0) \leq 0.05$	$-1.75 < SPI \leq -1.64$	1	0	0	0	0	6	5	4	0	3
$0.05 < F(0) \leq 0.06$	$-1.64 < SPI \leq -1.55$	1	0	0	0	0	1	2	2	0	3
$F(0) > 0.06$	$SPI > -1.55$	0	0	0	0	0	5	28	6	0	0

1013

1014

1015

1016 **Table 4.** Correlation between seasonal average p-value from the Shapiro-Wilk goodness-of-fit test and different catchment descriptors, for 121
1017 catchments. Correlations significant at the 5% level are shown in bold font.

	Catchment descriptor	1-month streamflow						1-month precipitation				
		Gamma	Generalized Logistic	GEV	Tweedie	Kappa3	Kappa4	Gamma	Pearson type 3	Tweedie	Kappa3	Kappa4
Winter	BFIHOST	-0.35	0.11	-0.10	-0.05	-0.05	-0.04					
	SMDBAR*	-0.26	-0.36	-0.56	-0.34	-0.37	-0.24					
	SAAR	0.44	0.27	0.45	0.15	0.34	0.35	0.03	0.17	0.03	0.10	0.15
	AREA	0.20	0.01	0.13	0.14	-0.02	0.12	-0.05	-0.03	-0.03	-0.09	0.14
Summer	BFIHOST	-0.05	0.46	0.23	-0.05	0.17	0.11					
	SMDBAR*	-0.35	0.05	-0.14	-0.32	-0.10	-0.43					
	SAAR	0.57	-0.31	0.00	0.34	0.06	0.34	-0.23	0.18	-0.11	0.33	0.15
	AREA	0.07	-0.05	0.04	0.10	-0.14	0.12	0.09	0.19	0.17	0.12	0.03

1018 * SMDBAR is only available for 31 catchments.

Figures with captions

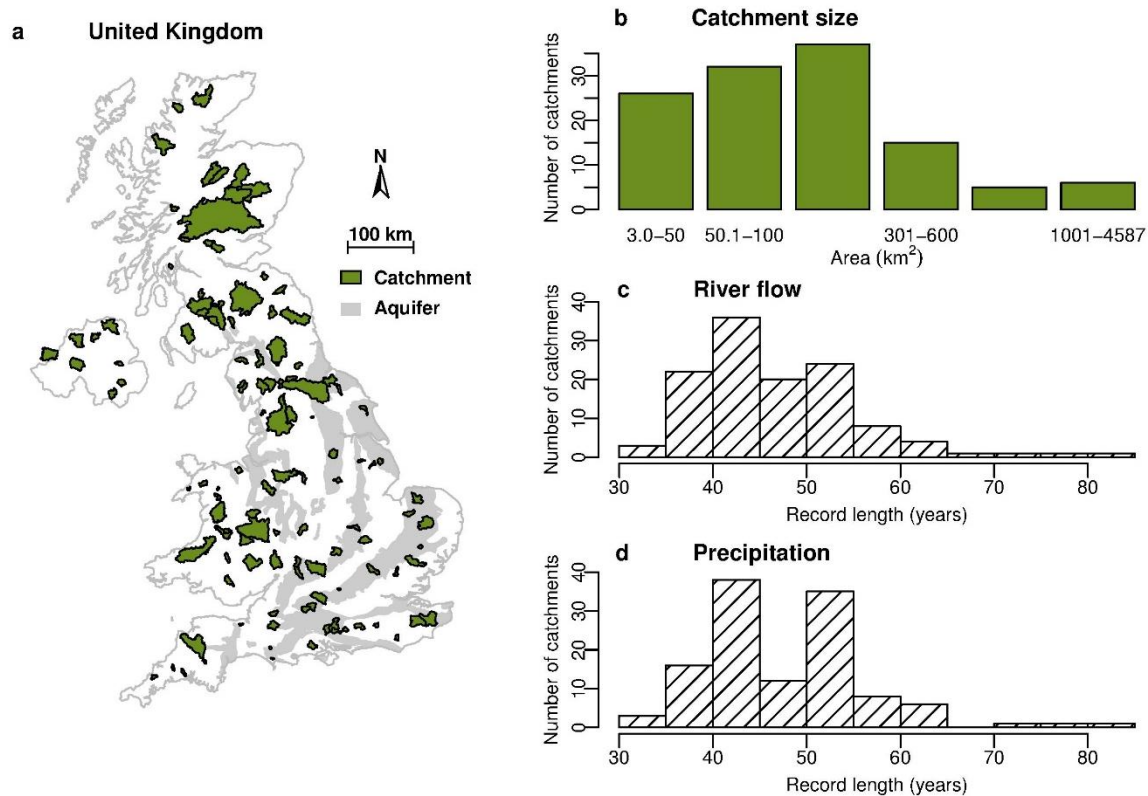


Figure 1. Location (a) and size (b) of the 121 study catchments in the UK. Record lengths excluding missing data for streamflow (c) and precipitation (d).

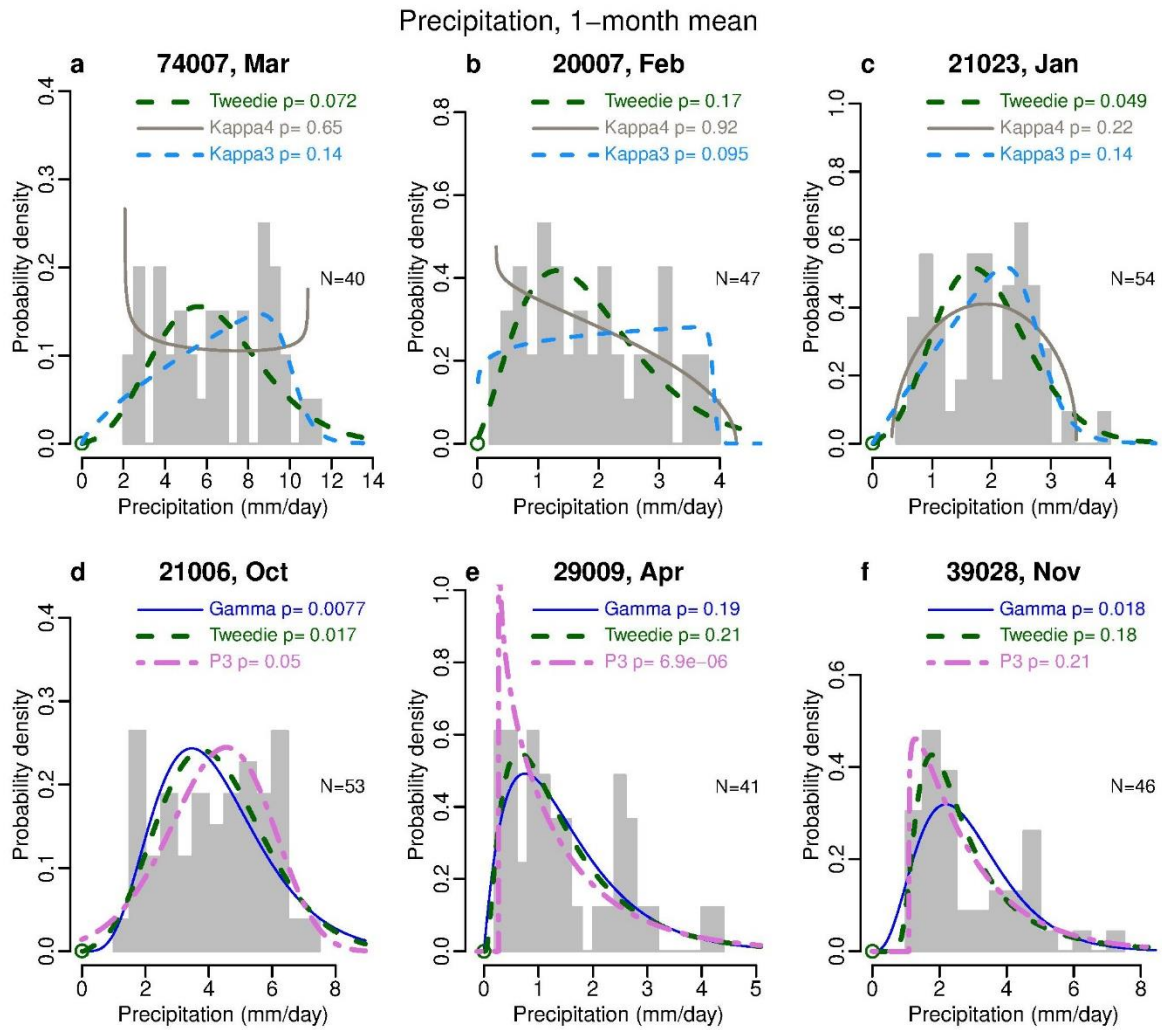


Figure 2. Examples of histograms of observed monthly mean precipitation and fitted probability density functions for a) Esk at Cropple How (hydrometric number 74007), b) Gifford Water at Lennoxlove (20007), c) Leet Water at Coldstream (21023), d) Tweed at Boleside (21006), e) Ancholme at Toft Newton (29009), and f) Dun at Hungerford (39028). The green circle shows the mass at zero for the fitted Tweedie distribution, which for convenience is shown on the same axis as the probability density function although it is a dimensionless probability between 0 and 1.

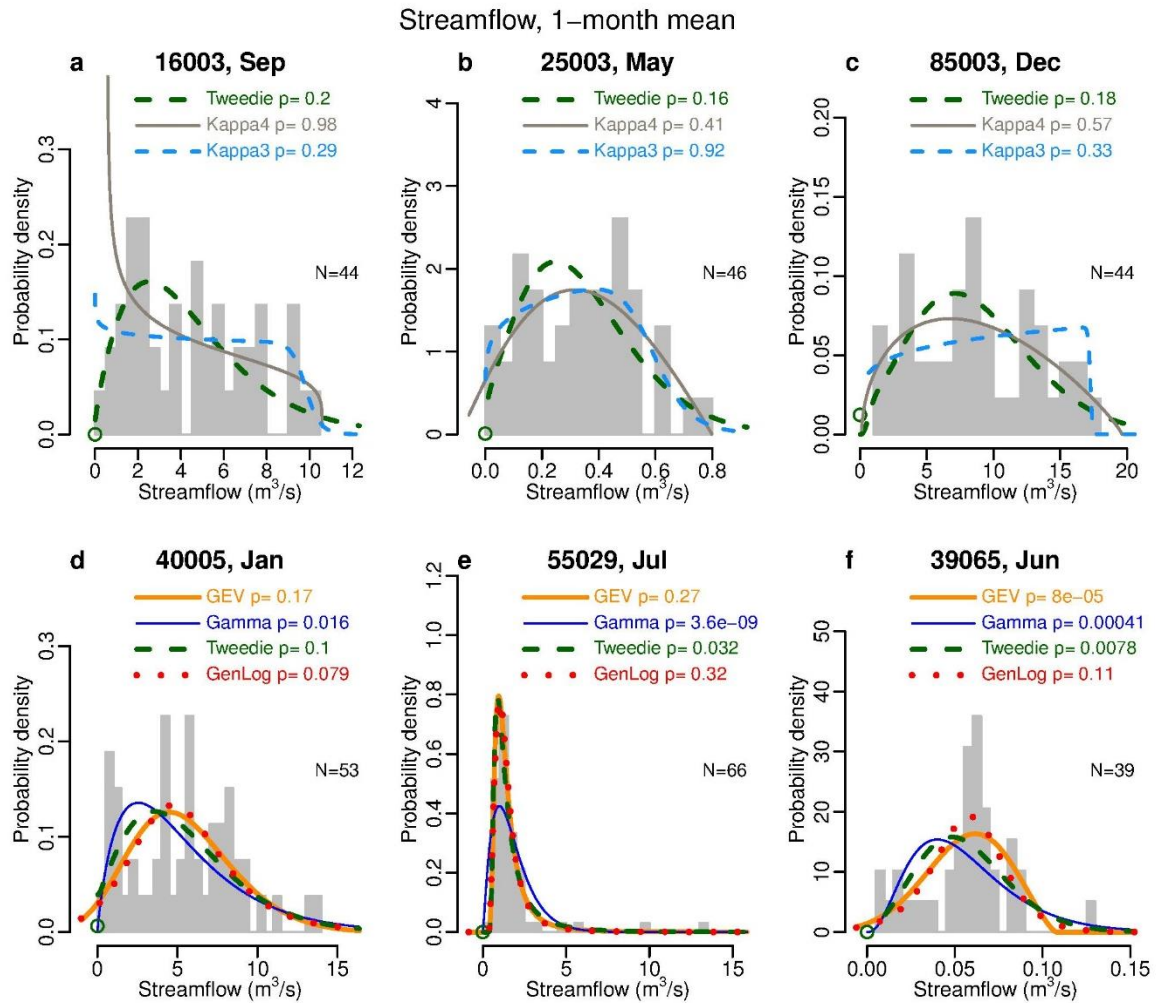


Figure 3. Examples of histograms of observed monthly mean streamflows and fitted probability density functions for a) Ruchill Water at Cultybraggan (hydrometric number 16003), b) Trout Beck at Moor House (25003), c) Falloch at Glen Falloch (85003), d) Beult at Stile Bridge (40005), b) Monnow at Grosmont (55029) and c) Ewelme Brook at Ewelme (39065). The green circle shows the mass at zero for the fitted Tweedie distribution, which for convenience is shown on the same axis as the probability density function although it is a dimensionless probability between 0 and 1.

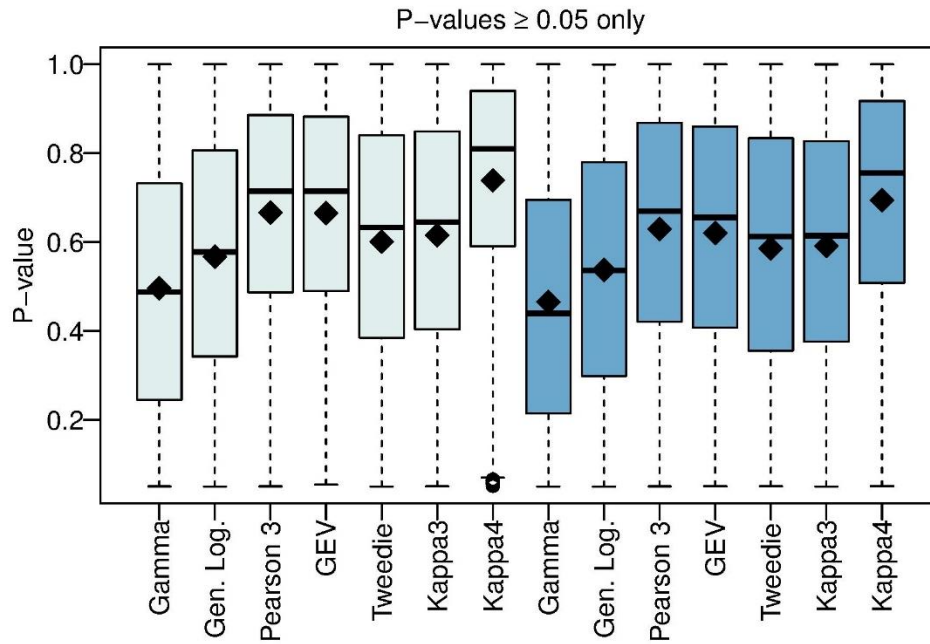


Figure 4. P-values for distributions accepted by the Shapiro-Wilk tests of normality for the SPI (light grey boxes) and SSI (blue boxes), for all 121 catchments, four aggregation durations, and 12 calendar end months lumped together. The box shows the inter-quartile range, the whiskers the maximum and minimum values, the thick line the median and the black diamond the mean of the p-values.

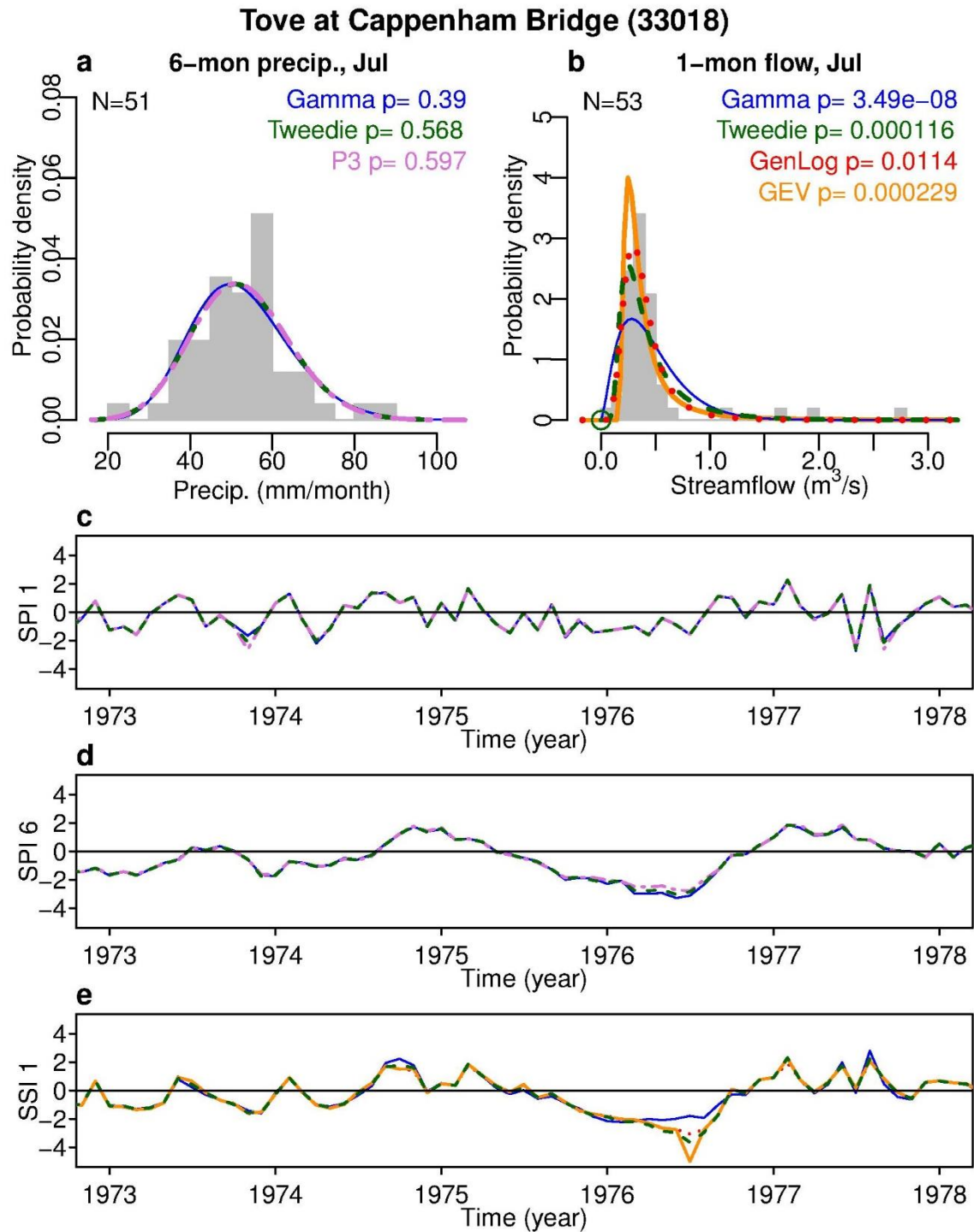


Figure 5. Effect of distribution choice on the calculated SPI and SSI. Example histograms and fitted distributions (see Figures 2 and 3 for line types) for a) 6-month mean precipitation, and b) 1-month mean streamflow for the Tove at Cappenham Bridge (hydrometric number 33018), and time series for the c) SPI 1, d) SPI 6 and e) SSI 1 drought indicators.

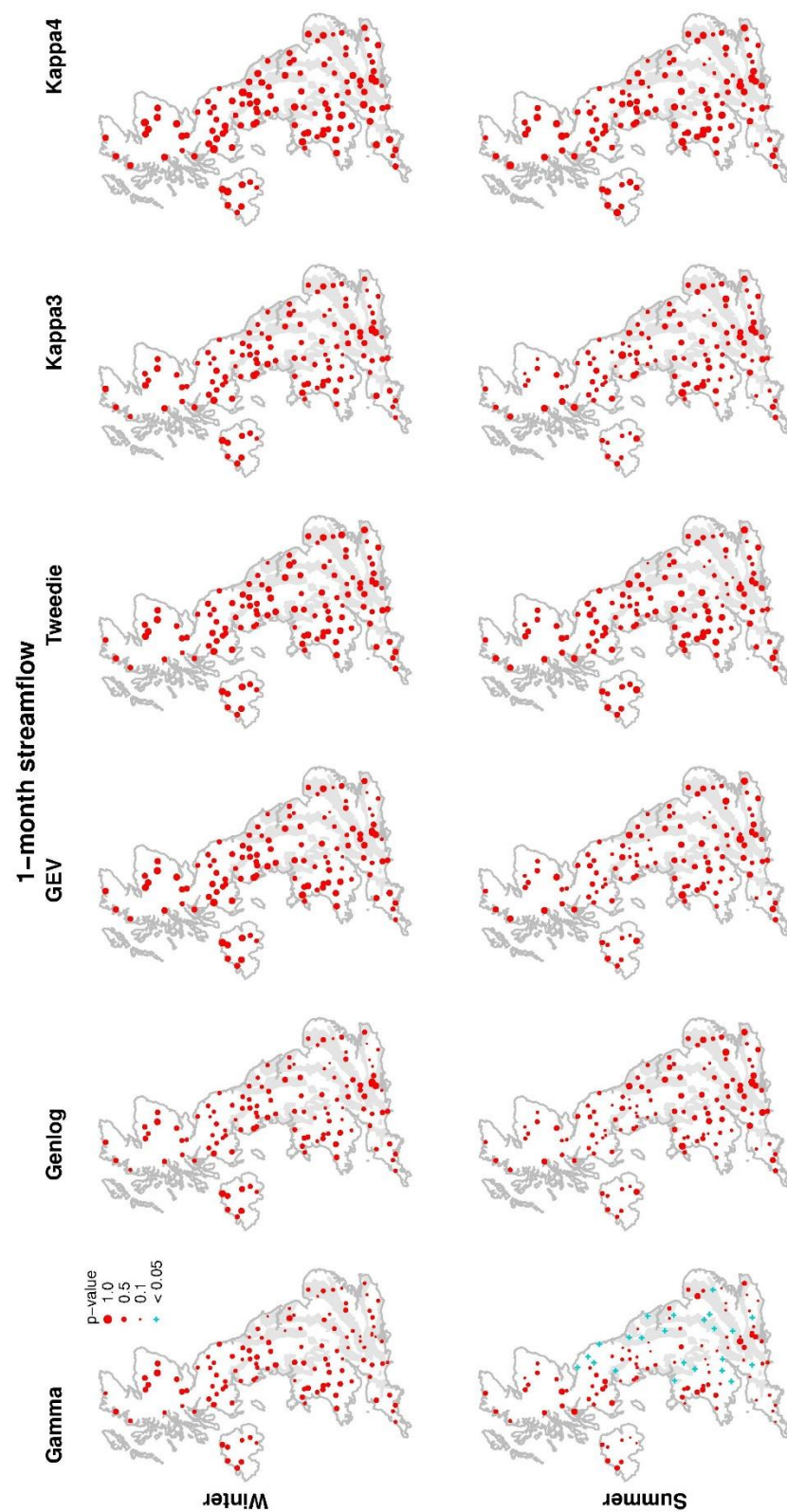


Figure 6. Seasonal average p-values for the Shapiro-Wilk goodness-of-fit test for SSI 1 at individual catchments, for a selection of distributions.